

CHAPTER IV

ANOMALOUS TRANSMISSION (BORRMANN EFFECT) IN ABSORBING CHOLESTERIC LIQUID CRYSTALS

1. Anomalous transmission of X-rays

This chapter is concerned with another striking phenomenon, namely, the anomalous transmission of light (or Borrmann effect) exhibited by absorbing cholesterics. Borrmann (1941) discovered a remarkable effect in the transmission of X-rays when a perfect absorbing crystal is set for Bragg reflection. Away from the Bragg setting, a crystal of sufficient thickness shows considerable reduction in the transmitted intensity due to photoelectric absorption. When it is set for Bragg reflection one expects a further reduction in the transmitted intensity as there is an additional loss due to reflection. Borrmann, using a quartz crystal of 0.2 mm thickness and FeK_α radiation, discovered an enhancement in the transmitted intensity instead of reduction. Also the transmitted ray had a slight lateral shift with respect to the

incident ray, instead of being **collinear** with it, in **such** a **way** that it appeared as though inside the **crystal** the energy travelled along the Bragg **planes**. This effect can be **explained** qualitatively as follows. **At** the Bragg **setting** **standing** waves are set up inside the medium due to the interference between the primary and Bragg reflected waves and **its** nature (**i.e.**, position of nodes and antinodes) depends on the phase difference between **the** two waves. When the medium is absorbing the phase difference **changes** and for **some angle** of incidence the **nodal** planes of the standing wave coincides with the atomic planes (figure 1). Therefore the atomic electrons see a reduced electric field and this results in a decrease of photoelectric absorption. Due to the **standing wave** nature, the component of the **Poynting** vector **normal** to the Bragg plane vanishes so that the energy flows parallel to the planes and this results in the slight **lateral** shift of the transmitted X-ray with respect to the incident ray.

This effect, in principle, **can** occur at any wavelength in an absorbing **system** **having** periodicity

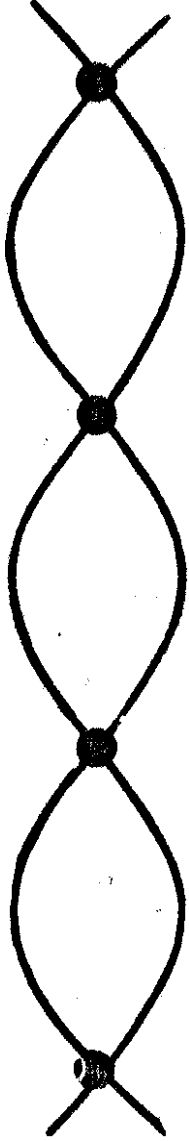


Figure 1: A qualitative picture of the Borrmann effect in X-rays. The nodes of the standing wave coincide with the atomic positions giving minimum absorption.

that **matches** with the wavelength of the incident radiation. But, so far, **an** optical analogue of **Bormann** effect **does** not appear to have been observed.

2. Anomalous transmission in cholesterics

For the occurrence of **this** effect, it may appear necessary to have a stratification of the absorption **centres** with **periodicity matching with** the wavelength of light. In **cholesterics** the wave sees a **continuously** twisted medium and the **reflected** circularly polarized wave has the **same** sense as that of the **incident** wave which will not result in a conventional standing wave consisting of **nodes** and **antinodes**. The **standing** wave pattern in **cholesterics** is of a different **type**; interference between the **reflected circularly polarized** light and the primary circularly polarized light of the **same** ^{sense} gives a **linearly polarized** wave whose **azimuth** rotates at the **same** rate as the director in the **medium**. The angle made by the **electric vector** of the **standing** wave with respect to the director depends on γ , the phase difference between the incident and

reflected right circularly polarized light. For a cholesteric of semi-infinite thickness ψ can be worked out as follows using dynamical theory.

From (10) in Chapter 3, the ratio of the amplitudes of the reflected and primary waves

$$\begin{aligned} \frac{S_0}{I_0} &= - \frac{iQ f_m(y) \exp(i\varphi)}{f_m(y) \exp(i\varphi) - f_{m-1}(y)} \\ &= - \frac{iQ}{1 - \frac{f_{m-1}(y)}{f_m(y)} e^{-i\varphi}} \end{aligned}$$

Now

$$\begin{aligned} \frac{f_{(m-1)}(y)}{f_m(y)} &= \frac{\sin h(m-1) \xi}{\sin h m \xi} \quad (\text{from equation 13, Chapter III}) \\ &= \cosh \xi - \coth m \xi \sinh \xi \end{aligned}$$

For a semi-infinite sample, $\cosh \xi = \coth m \xi \cdot \sinh \xi$
 $\approx \cosh \xi = \sinh \xi = e^{-\xi}$. Therefore

$$\frac{S_0}{T_0} = \frac{-1Q}{1 - e^{-1\varphi} \cdot e^{-\xi}} = \frac{-1Q}{1 - e^{-(1\epsilon + \xi)}} \quad (1)$$

$$\sim \frac{-1Q}{1\epsilon + \xi} = \frac{Q/\epsilon}{1 \pm \left[\frac{Q^2}{\epsilon^2} - 1 \right]^{\frac{1}{2}}} \cdot e^{-1 \pi/2}$$

(In the, reflection band ξ is real)

Separating this into an amplitude factor and a phase factor

$$\frac{S_0}{T_0} = \frac{Q/\epsilon}{\left[\frac{Q^2}{\epsilon^2} - 1 + 1 \right]^{\frac{1}{2}}} \cdot e^{-1 \pi/2} \cdot e^{-i \tan^{-1} \left\{ \pm 1 / \left[\left(\frac{Q^2}{\epsilon^2} - 1 \right) \right]^{\frac{1}{2}} \right\}}$$

Therefore

$$\psi = \frac{\pi}{2} \pm \tan^{-1} \frac{1}{\left[\frac{Q^2}{\epsilon^2} - 1 \right]^{\frac{1}{2}}} \quad (2)$$

The dependence of ψ on $\epsilon(\lambda)$ is given in figure 2.

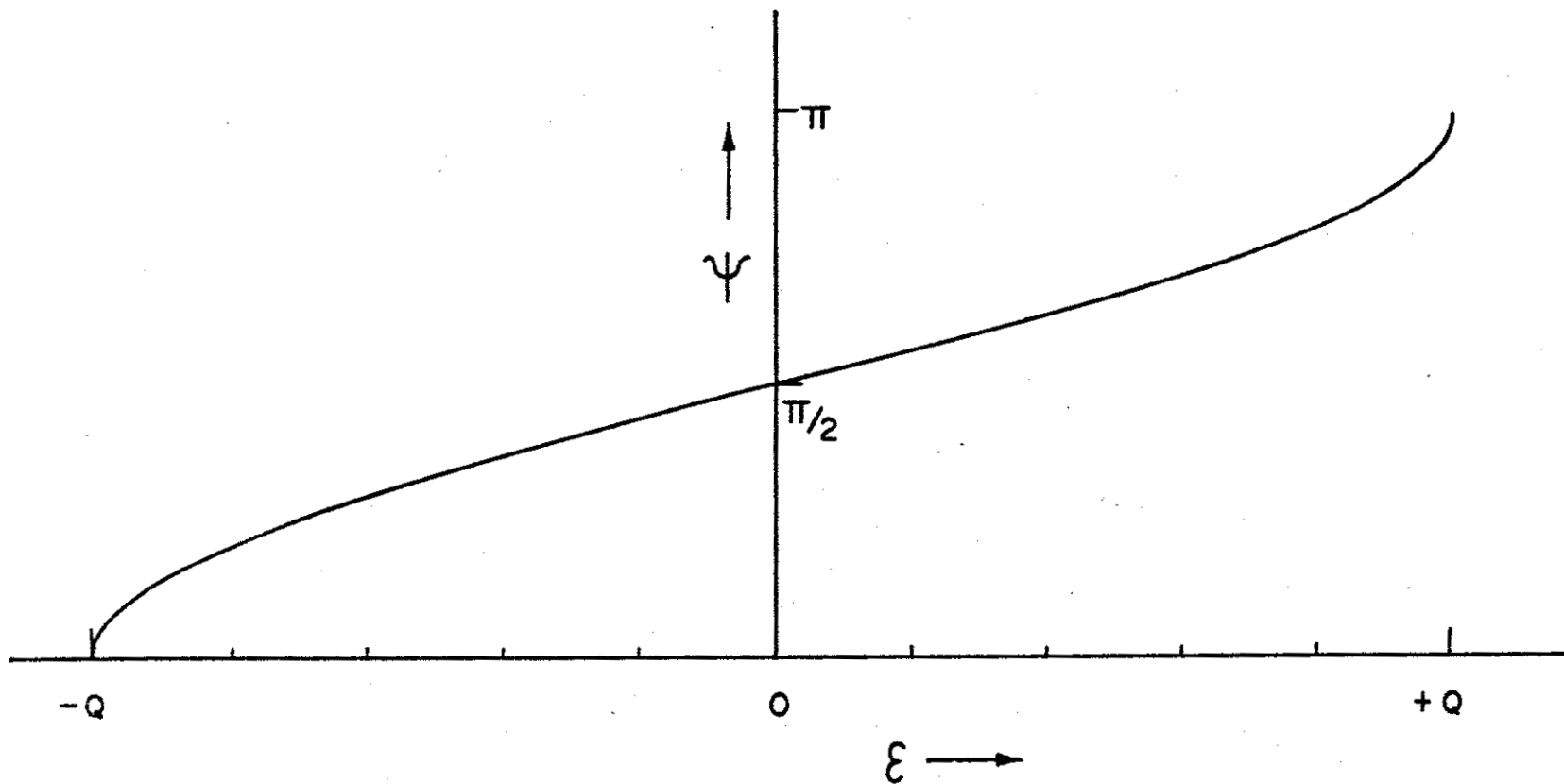


Figure 2 The phase of the reflected wave with respect to the primary wave plotted as a function of $\epsilon(\lambda)$.

When $\epsilon = Q, \gamma = \pi/2 + \pi/2 = \pi$

$$\epsilon = 0, \gamma = \pi/2 + 0 = \pi/2$$

$$\epsilon = -Q, \gamma = \pi/2 - \pi/2 = 0$$

Thus the phase of the reflected wave with respect to the primary wave varies from ' π ' to ' 0 ' starting from the shorter wavelength edge to the longer wavelength edge of the reflection band. Hence the electric vector in the medium makes an angle $\pi/2$ with respect to the director at the shorter wavelength edge and along the director at the longer wavelength edge. The refractive index and the absorption coefficient in the direction of the director (i.e., long axis of the molecule) is assumed to be greater than that in the direction perpendicular to it. Then the electric vector of the standing wave experiences minimum attenuation at the shorter wavelength side and maximum attenuation at the longer wavelength side of the reflection band. As a result of this, there occurs an anomalous increase in the transmitted intensity on the shorter wavelength side which is over and above the normal attenuation. One finds that in

cholesterics the optimum conditions to observe Borrmann effect are satisfied not exactly at the centre of the reflection band but at one edge of it, this being similar to the X-ray case where the effect occurs not at the Bragg angle but at a slightly different angle.

3. Dynamical theory of absorbing cholesterics

In this chapter the dynamical theory is applied to explain the Borrmann effect in absorbing cholesterics (Chandrasekhar et al. 1973). It is assumed that the layers are linearly dichroic in addition to being linearly birefringent and that the principal axes of the two coincide with each other. Therefore parameters like μ_{\pm} , Q , φ_R , φ_L become complex. If $\hat{\mu}_1$ and $\hat{\mu}_2$ be the principal complex refractive indices of each layer, then the reflection coefficient \hat{Q} and the phase retardation $\hat{\varphi}$ per pitch also become complex; i.e.,

$$\hat{Q} = \pi \frac{\Delta \hat{\mu}}{\hat{\mu}}$$

$$\hat{\varphi}_R = \frac{2\pi}{\lambda} \hat{\mu}_R P = \frac{2\pi}{\lambda} \hat{\mu} P - \frac{\pi(\Delta \hat{\mu})^2 P^2}{4\lambda^2}$$

$$\hat{\varphi}_L = \frac{2\pi}{\lambda} \hat{\mu}_L P = \frac{2\pi}{\lambda} \hat{\mu} P + \frac{\pi(\Delta \hat{\mu})^2 P^2}{4\lambda^2}$$

Here

$$\Delta \hat{\mu} = \hat{\mu}_1 - \hat{\mu}_2 \quad \hat{\mu}_1 = \mu_1 - ik_1$$

$$\hat{\mu} = \frac{1}{2}(\hat{\mu}_1 + \hat{\mu}_2) \quad \hat{\mu}_2 = \mu_2 - ik_2$$

k_1 and k_2 are the principal absorption coefficients.

All the equations obtained for non-absorbing media are still valid for absorbing systems excepting that \hat{Q} , $\hat{\varphi}_R$, $\hat{\varphi}_L$, $\hat{\mu}_R$, $\hat{\mu}_L$ replace Q , φ_R , φ_L , μ_R and μ_L respectively. For example, for a thick specimen, the reflection coefficient R for the right circular wave, the wave vectors \hat{k}_R and \hat{k}_L of the circular waves are given by

$$R = \left| \frac{\hat{Q}}{\hat{\epsilon} \pm (\hat{\epsilon}^2 - \hat{Q}^2)^{\frac{1}{2}}} \right|^2 \quad (3)$$

$$\hat{k}_R = \frac{2\pi + \hat{\xi}/1}{P}, \quad \hat{k}_L = \frac{(2\pi \hat{\mu}_L)}{\lambda} \quad (4)$$

Here

$$\hat{\epsilon} = \frac{2\pi}{\lambda}(\hat{\mu}_R P - \lambda)$$

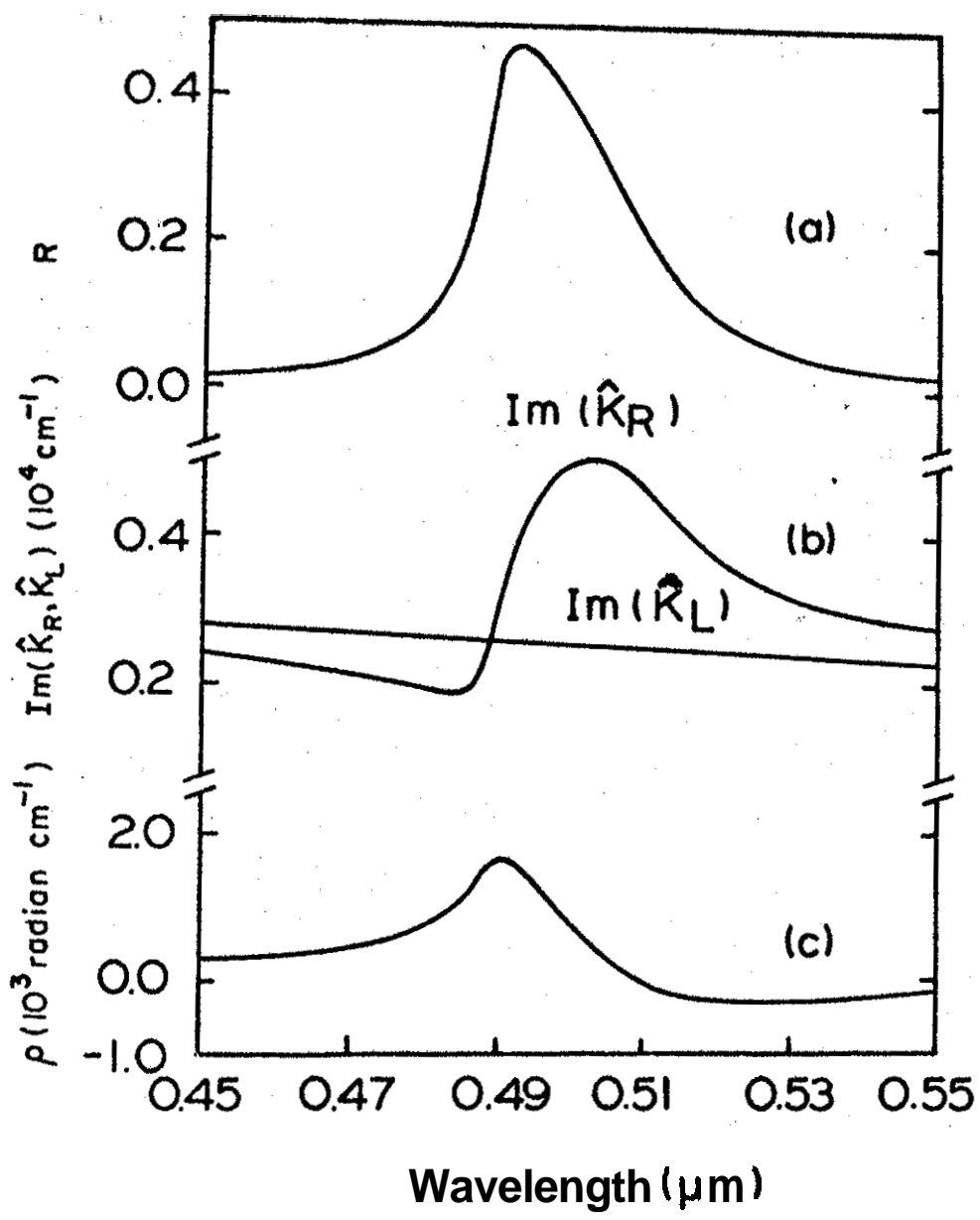
$$\hat{\kappa} = \pm (\hat{Q}^2 - \hat{\epsilon}^2)^{\frac{1}{2}}$$

Figure 3 presents the dependence of R , the imaginary parts of \hat{K}_R and \hat{K}_L on wavelength. Here $k = \frac{1}{2}(k_1 + k_2) = 0.02$ and $\Delta k = k_1 - k_2 = 0.028$. The interesting result is that on the shorter wavelength side $\text{Im}(\hat{K}_R)$ is less than $\text{Im}(\hat{K}_L)$, i.e., the right circular wave is less attenuated than the left circular wave, whilst on the longer wavelength side the opposite is true.

The transmitted intensities T_R and T_L for the right and left circular waves through an absorbing cholesteric film of thickness mP for unit incident intensity are given by

$$\begin{aligned}
 T_R &= \left| \frac{1}{\exp(i\hat{\epsilon}) \frac{\sinh m \hat{\kappa}_R}{\sinh \hat{\kappa}_R} - \frac{\sinh (m-1)\hat{\kappa}_R}{\sinh \hat{\kappa}_R}} \right|^2 \\
 &\approx \left| \frac{\text{cosech } m \hat{\kappa}_R}{i\hat{\epsilon} + \hat{\kappa}_R \coth m \hat{\kappa}_R} \right|^2 \\
 T_L &= \left| \exp(-m\hat{\phi}_L) \right|^2
 \end{aligned} \tag{5}$$

Figure 3: The calculated values of (a) reflection coefficient R , (b) imaginary parts of \hat{K}_R and \hat{K}_L , (c) rotatory power \mathcal{S} , plotted as functions of λ for an absorbing semi-infinite medium.

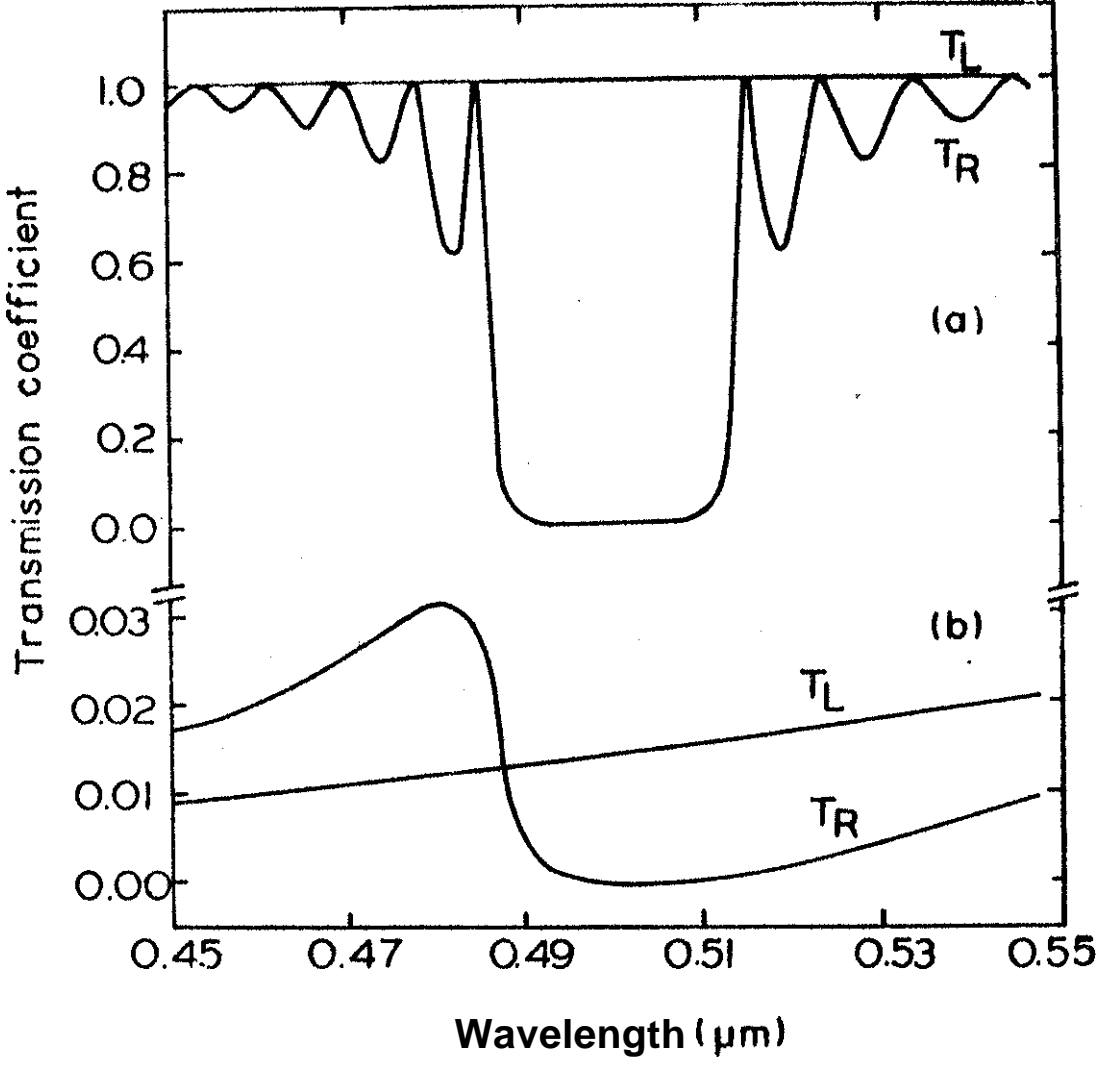


The theoretical dependence of T_R and T_L on wavelength are shown in figure 4 for both non-absorbing and absorbing cases for a film of thickness $25 P$. The structure being right-handed, the right circular component is reflected, and hence in the non-absorbing film ($k = \Delta k = 0$) T_R is always less than T_L . On the other hand, in the absorbing case, T_R has an enhanced value on the shorter wavelength side of the reflection band which is the Borrmann effect in cholesterics. It can be shown that T_L will exhibit an anomalous increase for a left-handed structure (i.e., negative β) and also that the enhanced transmission will occur on the longer wavelength side of the reflection band if Δk is negative.

4. Experiments

To observe the optical analogue of Borrmann effect in a cholesteric the molecules (layers) should have a linearly dichroic band in the visible region and this intrinsic absorption band should be wider than the Bragg band. Normally the compounds that exhibit cholesterio texture do not absorb in

Figure 4: The transmitted intensities T_R and ~~See~~ T_L for right and left circular waves (for unit incident intensity) for a film of thickness $25P$ (a) now absorbing, (b) absorbing. The enhanced transmission for the right circular component in (b) is the analogue of the Borrmann effect.



the **optical** region. However, as explained in Chapter II, **it** is possible to induce linear dichroism in the **layers in a cholesteric** by dissolving linearly dichroic molecules (Saeva and **Wysokhi** 1971). The solute molecules arrange themselves **locally** in the order prevalent in the **medium** and therefore determine the absorption and **linear dichroic properties** of the medium.

Experiments were carried out on thin films of **cholesteryl nonanoate in which** was dissolved small quantities of **p-azoxyanisole (PAA)** or **n-p-methoxybenzylidene-p-phenylazoaniline (MBPAA)** (**Nityananda et al.** 1973, **Suresh** 1976). PAA and MBPAA have strong linearly dichroic bands around **0.36 μm** and **0.38 μm** respectively. Pure cholesteryl nonanoate is left handed and has a Bragg reflection band at **0.36 μm** at **88.5°C**. The temperature corresponding to the **Bragg** reflection band **0.36 μm** **decreases** slightly with addition of **small** quantities of either PAA or MBPAA. The mixture is **also** left handed and **reflects** left **circularly polarized light** at the **reflection band**. The experimental procedure is to adjust the sample temperature so

that the reflection band of the **cholesteric** mixture coincide (as closely as possible) with the absorbing band of the **solute molecules**.

The sample was taken between two **optically flat** ($\sim \lambda/10$) **fused silica** plates and by careful **displacement** of the plates well oriented plane texture **cholesteric** could be obtained. The **thickness** of the **sample** and the **concentration** of the **solute molecules** play an **important** role in observing **Borrman** effect. A thick **sample** does not give well oriented **specimen** by over slip displacement and a very thin sample **does** not have sufficient number of pitches to give a well defined Bragg reflection. **Also** a very **small** percentage of the solute molecules will not **show** the effect prominently and on the other hand a high percentage of the solute **molecules** does not transmit any **detectable** intensity. By **trials** it was found that a **sample thickness** of about $6 \mu\text{m}$ and solute **concentrations** in the range 1 to 4 per cent are suitable to observe the effect. In all the experiments the **sample thickness** was fixed using a mylar spacer of thickness 0.25 mil ($\approx 6.4 \mu\text{m}$).

A parallel beam of intense white light from a tungsten lamp was passed through a circular polariser and the sample. The transmission spectrum was recorded photographically using a quartz spectrograph (Hilger E 498.305/49645). The spectra for left- and right-circularly polarised light were recorded on the same photographic plate (one above the other) under identical conditions (see figure 5). Microdensitometer tracings were then obtained from the developed plates and the relative intensities were evaluated using previously calibrated relative intensity-density curves for the source spectrum. The relative intensities thus evaluated give a measure of the transmission coefficient of the sample. The constant of proportionality involved in the relative intensity was eliminated by calculating the circular dichroism defined as

$$D = \frac{T_L - T_R}{T_L + T_R + 2(T_L T_R)^{\frac{1}{2}}} \quad (6)$$

where T_L and T_R are transmitted intensity for left-

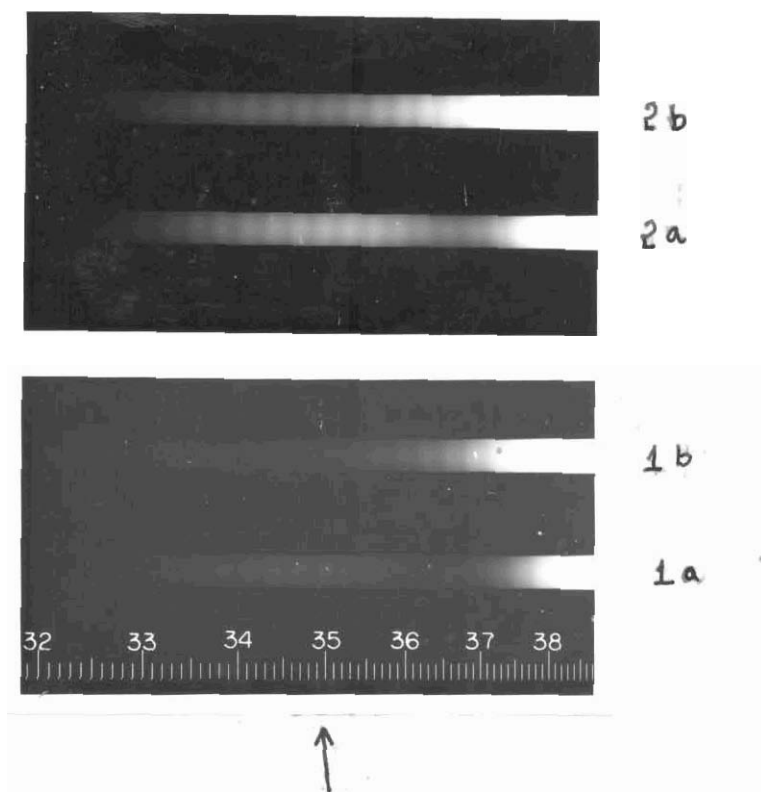


Figure 5

A typical transmission spectrum showing the Borrmann effect: (1) for a short exposure time, (2) for a longer exposure time. In both the cases 'a' is for the left circular wave which exhibits anomalous transmission, and 'b' is for the right circular wave which undergoes normal attenuation. The fringes are due to the channelled spectrum of the quarter wave plate. The wavelength scale is also given in the same plate. The reflection band is around 3600 \AA . 3hr region of enhanced transmission in 'a' is indicated by the arrow.

and right-circularly polarized light respectively.

The raw microdensitometer traces for non-absorbing sample are presented in figure 6. The two traces do not cross, indicating that the circular dichroism does not change sign. Figure 7 gives the two traces for 2.45% PAA (by weight) in cholesteryl nonanoate. For this composition, the maximum value of $\Delta k = 0.03$. The Bragg reflection occurs at about $0.355 \mu\text{m}$, as indicated by the dip in the transmission for left circular light. At shorter wavelengths, the transmission has actually risen above that for right circular light. Figure 8 gives the transmitted intensities (in arbitrary units) and figure 9 gives the circular dichroism for the same sample. Figure 10, 11 and 12 present the results of a similar experiment on 4.25% MBPAA, the Bragg reflection being at about $0.4020 \mu\text{m}$.

In interpreting the experimental transmitted intensity curve (figure 8) one must recall that the linear dichroism Δk is a function of wavelength having a maximum and falling off on either side. Since the experimental curves (figure 8)

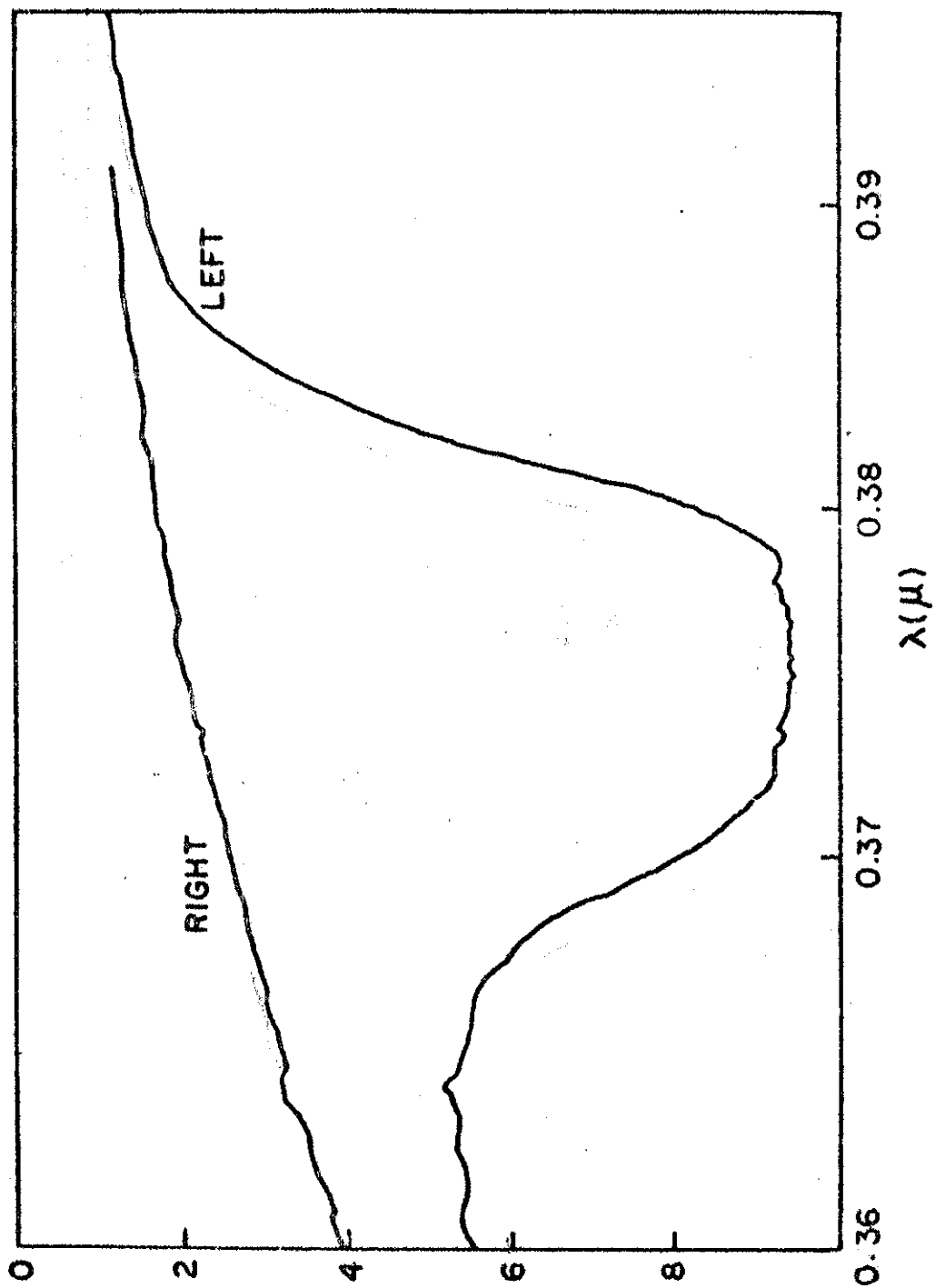
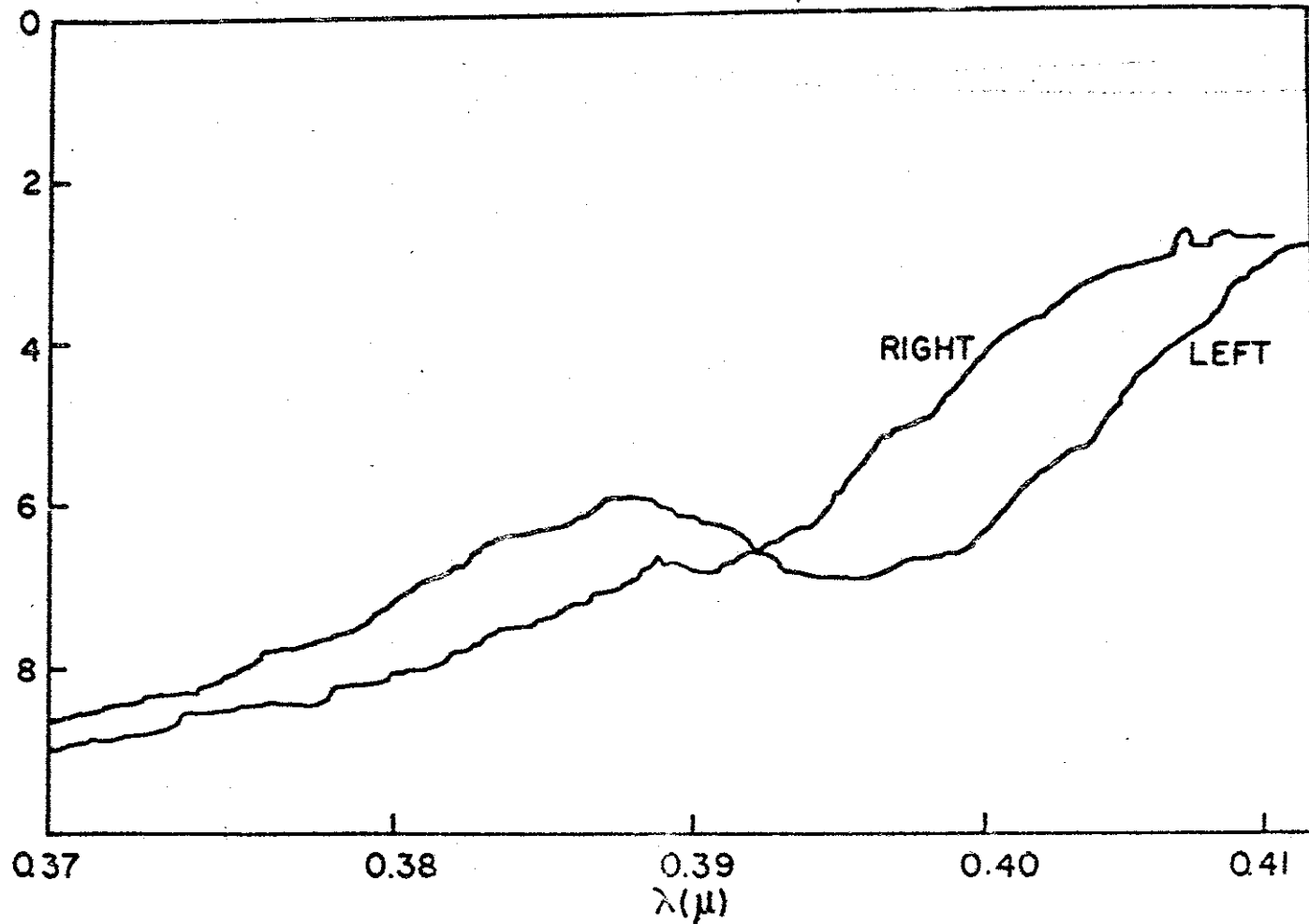


Figure 6: Raw microdensitometer traces for a non-absorbing sample (purr cholesteryl nonanoate) showing qualitatively the behaviour of the transmitted intensity as a function of wavelength for the two circular polarisations. Sample thickness $\approx 6.4 \mu\text{m}$.



**Figure 7: Microdensitometer traces for the two circular polarisations.
Sample: 2.45% PAA in cholesteryl nonanoate.**

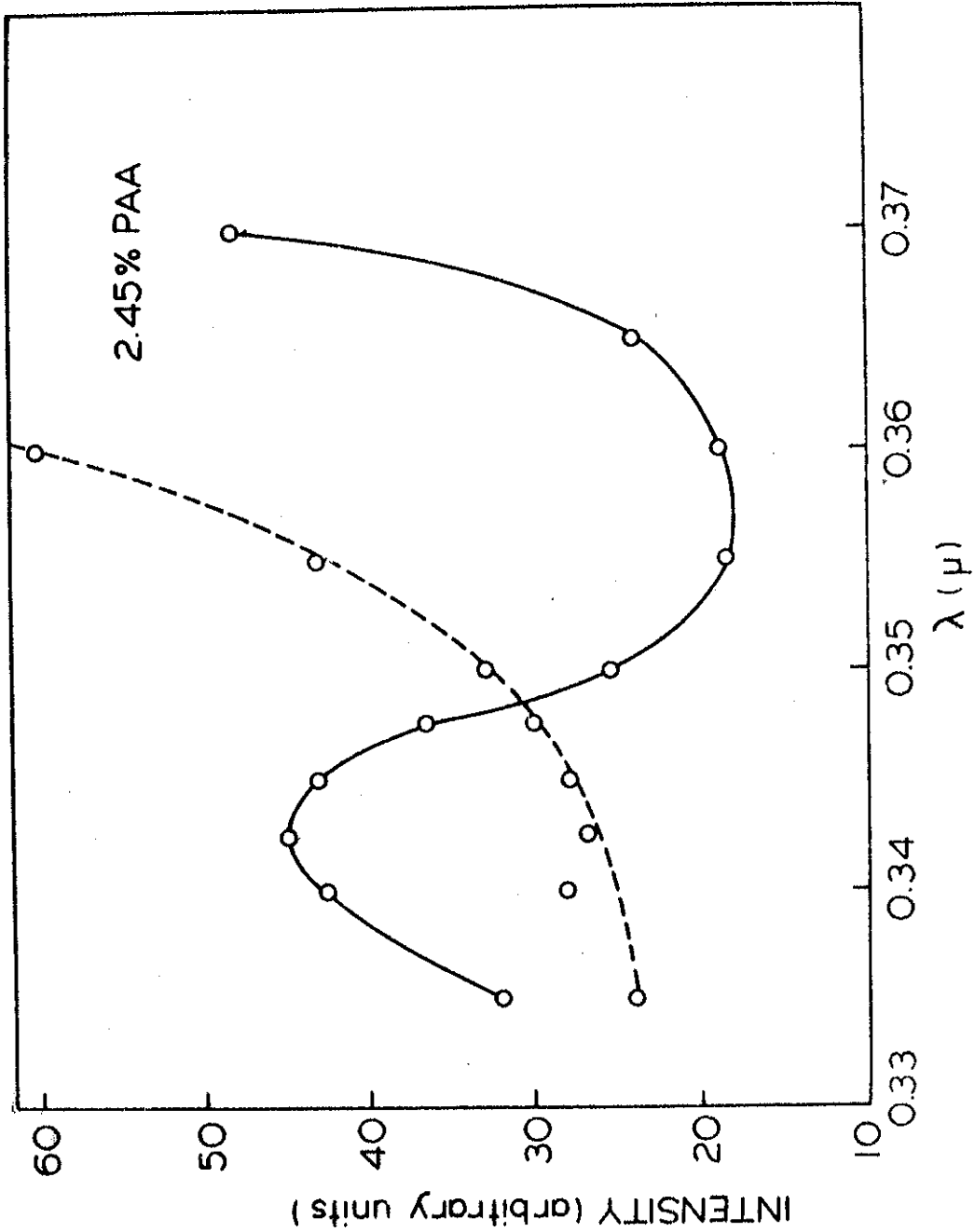


Figure 8: Transmitted intensity for the two circular polarisations (arbitrary units). The dashed line is for right circular polarisation and the solid line for left circular.

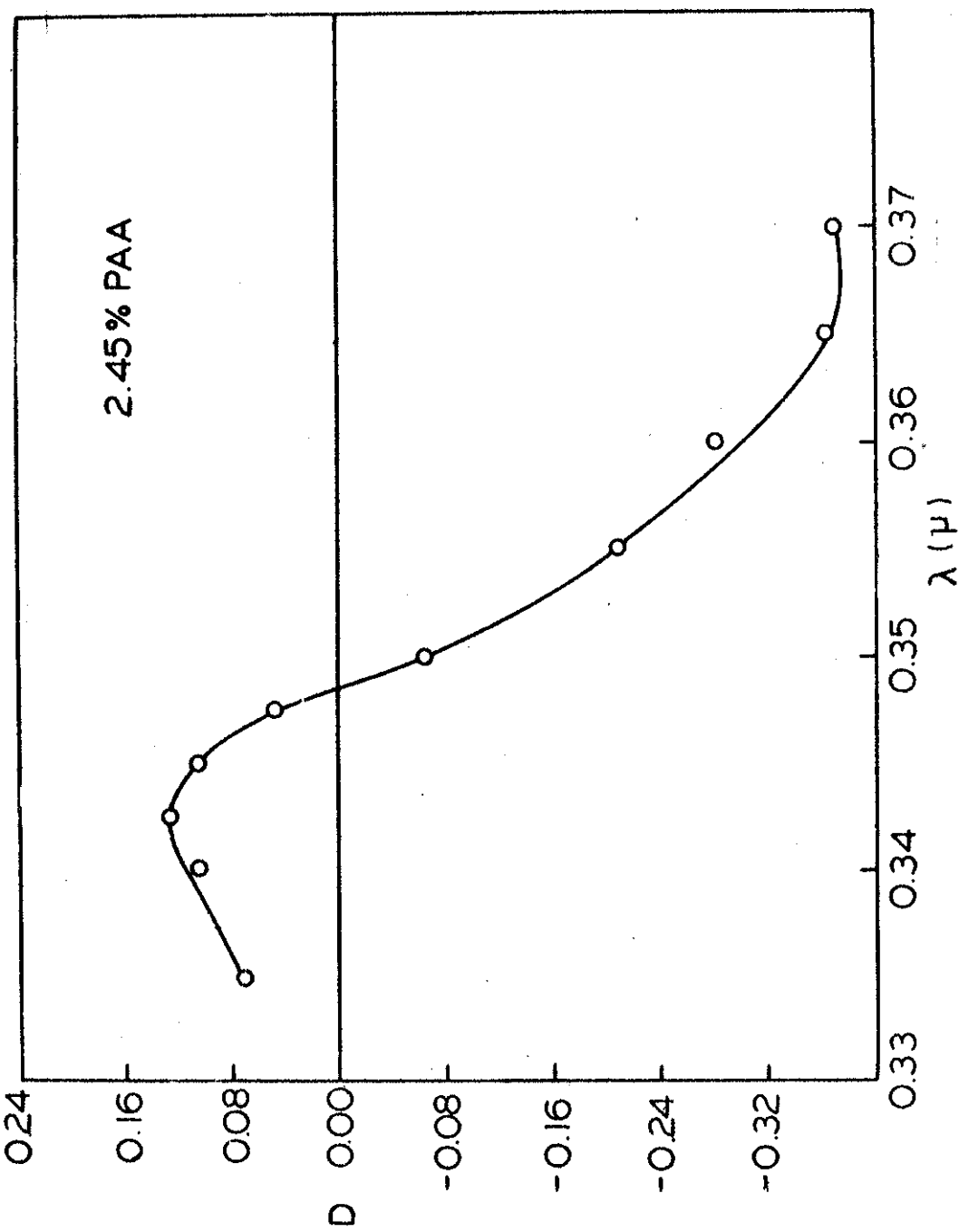


Figure 9: Circular dichroism as a function of wavelength for a sample of thickness $\approx 6.4 \mu\text{m}$.

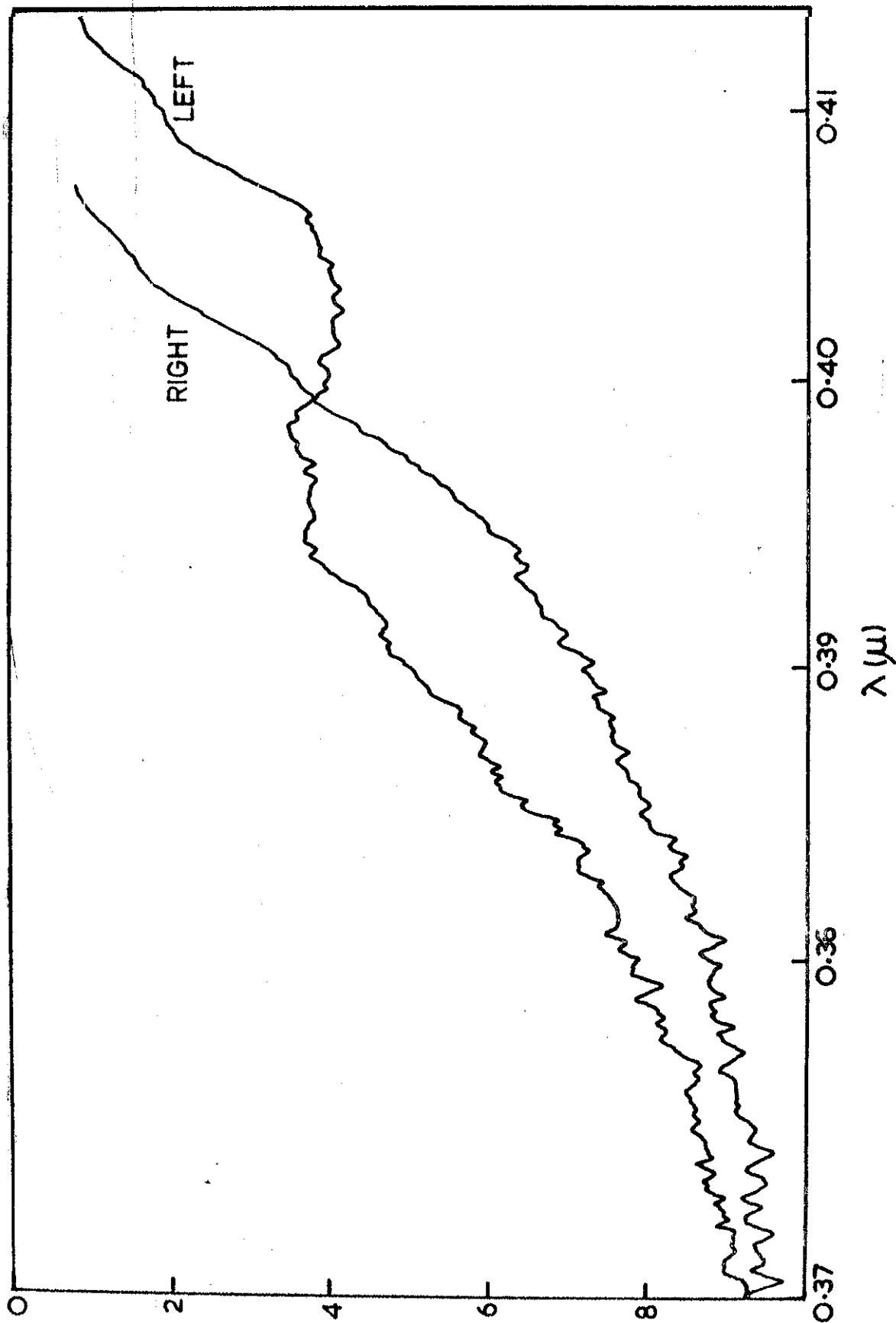


Figure 10: Microdensitometer traces for the two circular polarisations.

Sample: 4.25% MBPAA in cholesterol nonanoate.

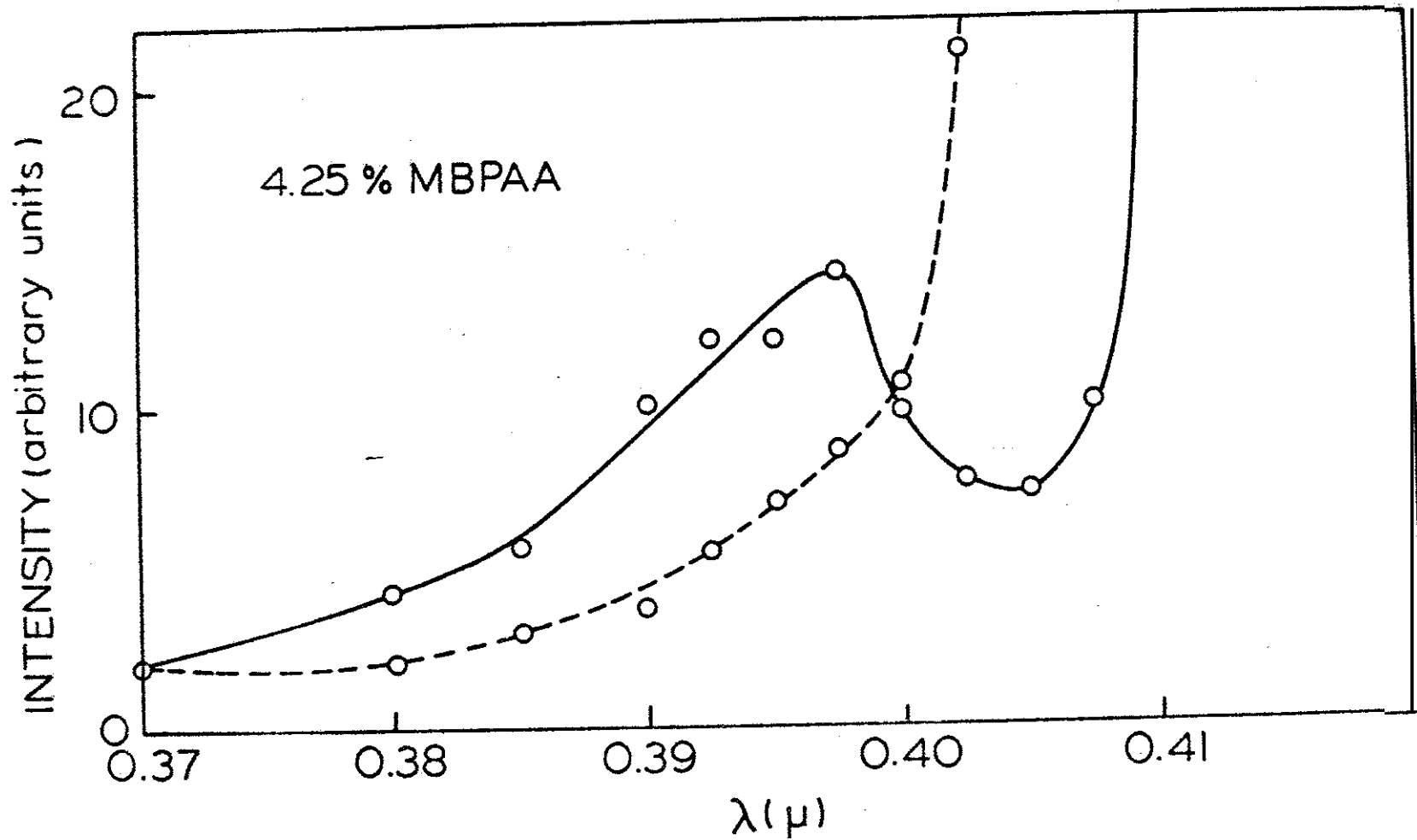


Figure 11: Transmitted intensity in arbitrary units as a function of wavelength. The dashed line is for right circular polarisation and the solid line for left circular.

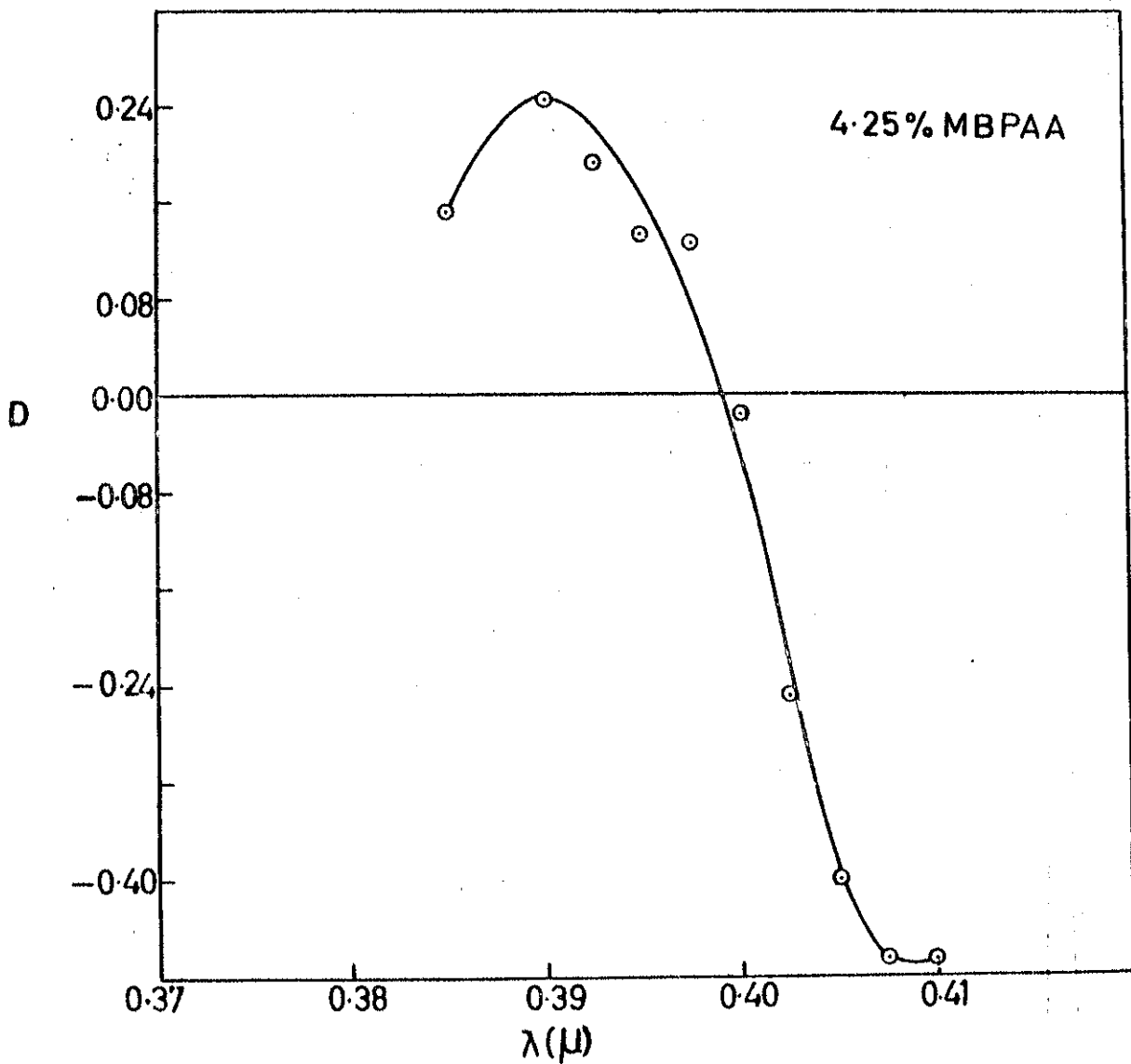


Figure 12: Circular dichroism as a function of wavelength for a sample of thickness $\approx 6.4 \mu\text{m}$.

depend **critically** on the relative position of the reflection band **and** on the linearly **dichroic** band of the eolute moleculee, one **does not expect** it to resemble **very closely** the **theoretical curves** (figure 4) **computed** for conetant Δk . However, the **circular dichroism curves** (Figures 9 and 12) do ehow a **positive maximum** at shorter wavelengths which falls off st longer **wavelengths**, **characteristic** of the **Borrmann effect**.

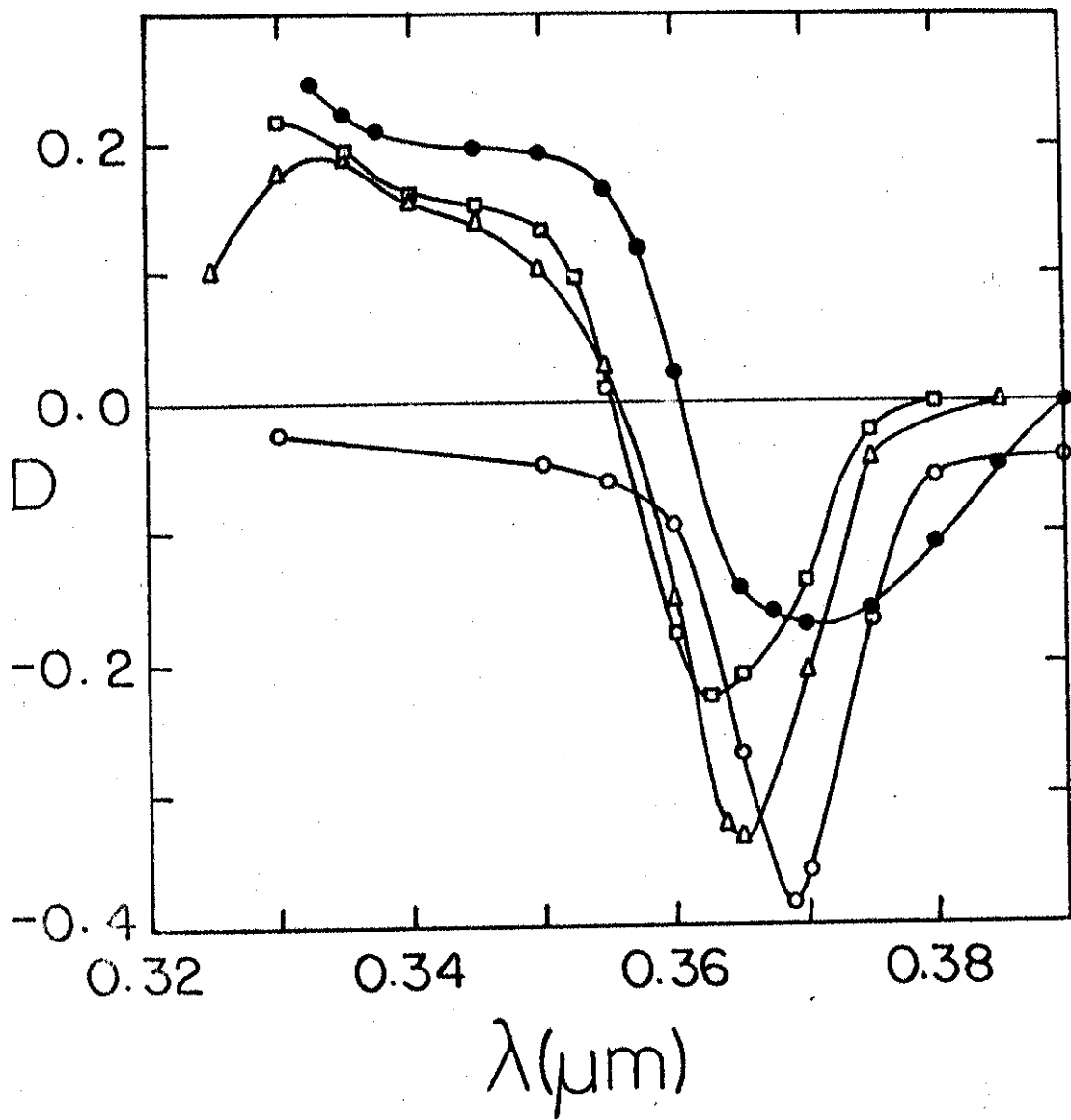
5. Dependence of anomalous transmission on the concentration of eolute molecules.

With a view to making a more **detailed comparison** with the theory we shall now present studies carried out on thin **films** of **mixtures** of **cholesteryl nonanoate** and **p-azoxyanisole (PAA)** of different **concentrations**. **PAA** was used because the **polarized ultraviolet absorption spectra** of this **compound** have been reported (**Maier and Saupe 1956**) from which k and Δk could be **evaluated** and used in the **theoretical calculations**. All **experiments** were performed on **films** at **thickness** $6.4 \mu\text{m}$ (with **mylar spacers** of **0.25 mil**). The **sample** was prepared by

the **method** explained in section 4. The **light source** was **aniodine-quartz** lamp which has high intensity **down** to $0.3 \mu\text{m}$. The position of the reflection band of the medium with respect to the absorption band of the solute molecules is very **critical** in determining the **anomalous transmission** profile. With **increase** in the concentration of PAA, **it** becomes more and more **difficult** to **locate** the centre of the reflection band **since** the setting in of the **anomalous** transmission alters the shape of the normal **Bragg** reflection profile. **Moreover** the reflection band itself depends on the **concentration** of PAA and on the temperature. The **position** of the reflection band, located by the **minimum** in the **transmission spectrum**, was adjusted (as closely as possible) to **coincide** with the absorption band of the **solute molecules** by varying the **temperature**. To **evaluate** the **transmitted** intensities and **circular dichroism** D , the same method described in **section 4** was followed.

Figure 13 presents experimental curves of D as a function of wavelength for 0, 0.98, 1.76 and

Figure 13: Experimental curves of circular dichroism as a function of wavelength for mixtures of cholesteryl nonanoate and PAA. Non-absorbing (0% PAA),
 ○ ○ ○ - Absorbing (1) 0.98% PAA,
 △ △ △ - (2) 1.76% PAA, □ □ □ -
 (3) 3.78% PAA, ● ● ●



3.78% PAA (by weight) concentration. The curves give the following features:

- a. In absorbing cholesterics, D changes sign at the lower wavelength side of the reflection band, whereas for the non-absorbing cholesterics (0% PAA) D is always negative.

The change of sign in D for the absorbing case is due to the anomalous transmission of the left circularly polarised light which is enhanced at the lower wavelength side and attenuated at the higher wavelength side of the reflection band. The right circularly polarised light buffers only the normal attenuation,

- b. With increase in the concentration of PAA the magnitude of the negative peak decreases while the positive side indicates an increasing trend.
- c. The half width of the negative peak increases with increasing PAA concentration.

6. Comparison with theory

In section 3 while writing down the equations for anomalous transmission it was assumed that the absorbing system is a right handed cholesteric whereas the cholesteryl nonanoate and PAA mixture used in the experiments adopt a left handed helix. Here the left circularly polarised light undergoes Bragg reflection and anomalous transmission. From (5) the transmitted intensities of the left- and right-circularly polarized light are given by

$$T_L = \left| \frac{\hat{\xi} \operatorname{cosech} m \hat{\xi}}{i\hat{\epsilon} + \hat{\xi} \coth m \hat{\xi}} \right|^2 \quad (7)$$

$$T_R = \left| \exp(-m\hat{\phi}_R) \right|^2$$

where m = number of pitches in the sample thickness. Using equations (7) and (6) the theoretical values of D versus wavelength were computed. The above calculations were made on a IBM 360 computer using Fortran IV language. (I am grateful to Dr. G.S.

Ranganath for his help in writing the computer programme.) The absorption coefficients of the cholesteryl nonanoate + PAA mixture around $0.36 \mu\text{m}$ were assumed to be only due to that of PAA. The molecular extinction coefficient ϵ for PAA in the isotropic phase ($\bar{\epsilon}$) and in the nematic phase for the electric vector polarised perpendicular to the director (ϵ_{\perp}) were taken from ^{the data of} Maier and Saupe (1956). The maxima of absorption in the two cases are at 0.34 and $0.355 \mu\text{m}$ respectively. ϵ is related to the absorption coefficient k by the general equation

$$k = 2.303 \epsilon c / 2\pi$$

where c = concentration of PAA, λ = wavelength of Light. The absorption profiles were fitted approximately to a Gaussian of the form

$$= k_{\text{max}} \cdot \exp \left[- \left(\frac{\lambda - \lambda_{\text{max}}}{\Delta\lambda} \right)^2 \right]$$

Using the experimental values of $\bar{\epsilon}$ and ϵ_{\perp} along with the above expressions, $k = \frac{1}{2}(k_1 + k_2)$ and $\Delta k = (k_1 - k_2)$ were calculated as a function

of wavelength and concentration. The other parameters used in the calculations were $P = 0.24 \mu\text{m}$, $\lambda_0 = \mu P = 0.36 \mu\text{m}$ (i.e., $\mu = \frac{\mu_1 + \mu_2}{2} = 1.5$), $m = 25$ and $\Delta\mu = 0.07$. The dispersion of μ and $\Delta\mu$, as well as the dependence of k and Δk on temperature were neglected. Theoretical curves of D computed for a few typical values of k and Ak are presented in Figure 14.

To check the theory quantitatively is difficult owing to experimental difficulty of adjusting the reflection band to coincide exactly with the absorption band of the molecules. A slight deviation can drastically change the anomalous transmission profile. For example the Borrmann effect is less prominent in Figure 9 than in Figure 13 for comparable concentrations of PAA since in the preliminary experiments (Figure 9) the reflection band was not as carefully adjusted to coincide with the absorption band of the solute molecules as in the case of the later experiments (Figure 13). Ideally, the experiment should have been performed with solute molecules with a very broad linearly dichroic absorption band, but there

Figure 14: Theoretical curves of circular dichroism as a function of wavelength for a few values of k and Δk .

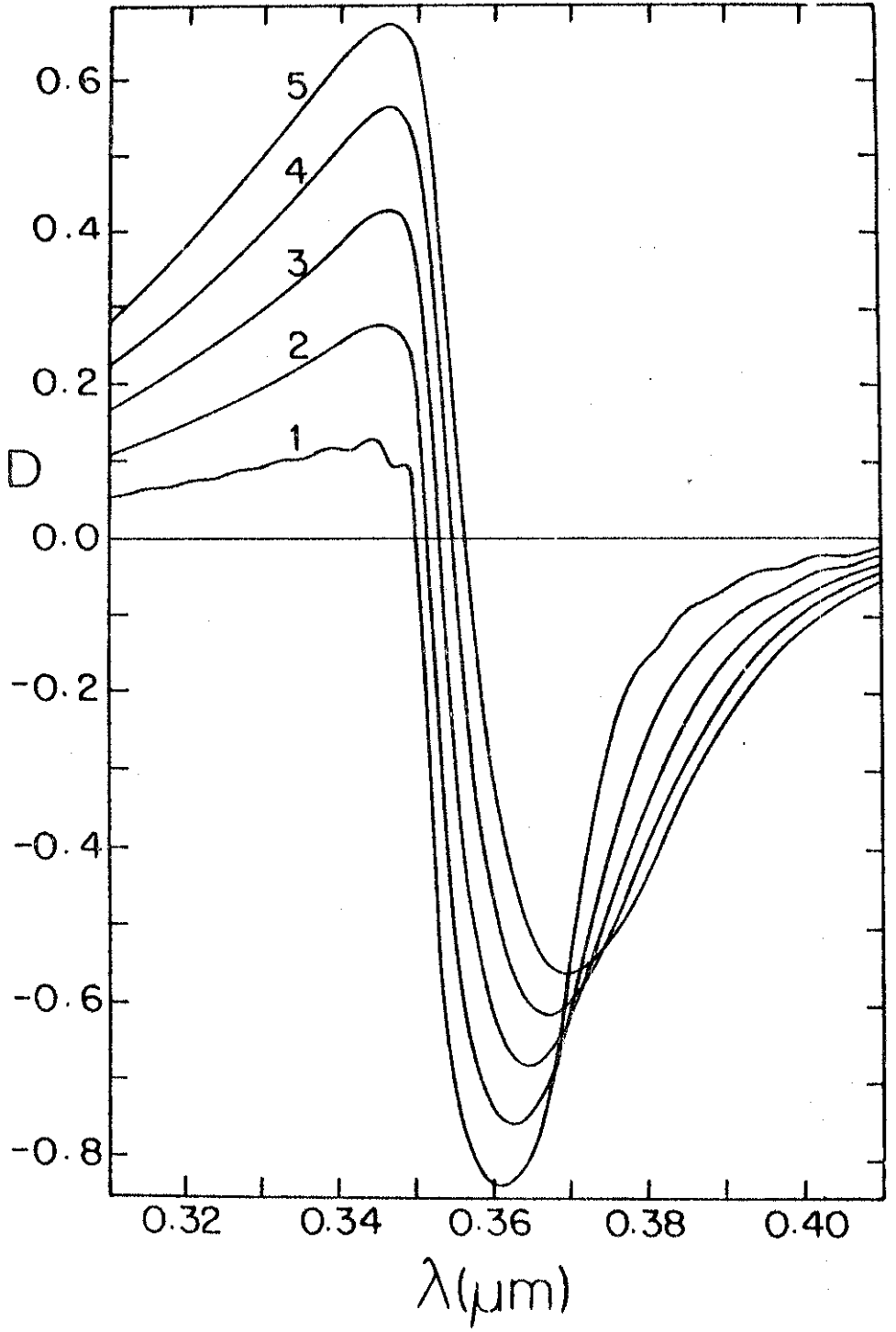
1) $k = 0.0125$, $\Delta k = 0.0157$ (1% PAA)

2) $k = 0.0250$, $\Delta k = 0.0314$

3) $k = 0.0375$, $\Delta k = 0.0471$

4) $k = 0.0500$, $\Delta k = 0.0628$

5) $k = 0.0625$, $\Delta k = 0.0785$



are few euah rnoleoulea. Nevertheless, **it is** gratifying that there **is** qualitative agreement between experiment and theory. In particular the prediction that with **increasing** oonoentrstion of PAA, the **positive peak** in the **circular dichroism curve should increase** in magnitude and the negative peak should **decrease** in magnitude but increase in **half width is** borne out by **experiments.**

Referenae

Borrmann, G. 1941 Z. Phys. 42, 157

Chandrasekhar, S., Ranganath, G.S. and Suresh, K.A.
1973 Proceedings of the International Liquid
Crystals Conferenoe, Bangalore - Pramana Suppl.
1, 341.

Mafer, W. and Saupe, A. 1956 Z. Physik. Chem. (NF)
6, 327.

Nityananda, R., Kini, U.D., Chandrasekhar, S.
and Suresh, K.A. 1973 Proceedings of the
International Liquid Crystals Conference, Bangalore -
Pramana Suppl. 1, 325.

Saeva, P.D. and Wysocki, J.J. 1971 J. Amer. Chem.
Soa. , 5928.

Suresh, K.A. 1976 Mol. Cryst. Liquid Cryst. 35,
267.